PHYSICAL REVIEW B **96**, 180408(R) (2017)

# Spin-orbit coupling fluctuations as a mechanism of spin decoherence

M. Martens,[1,2,*] G. Franco,[1,2] N. S. Dalal,[2,3] S. Bertaina,[4] and I. Chiorescu[1,2,†]
[1]*Department of Physics, Florida State University, Tallahassee, Florida 32306, USA*
[2]*The National High Magnetic Field Laboratory, Tallahassee, Florida 32310, USA*
[3]*Department of Chemistry and Biochemistry, Florida State University, Tallahassee, Florida 32306, USA*
[4]*Aix-Marseille Université, CNRS, IM2NP UMR7334, 13397 cedex 20, Marseille, France*
(Received 24 August 2017; published 14 November 2017)

We discuss a general framework to address spin decoherence resulting from fluctuations in a spin Hamiltonian. We performed a systematic study on spin decoherence in the compound $K_6[V_{15}As_6O_{42}(D_2O)] \cdot 8D_2O$, using high-field electron spin resonance. By analyzing the anisotropy of resonance linewidths as a function of orientation, temperature, and field, we find that the spin-orbit term is a major decoherence source. The demonstrated mechanism can alter the lifetime of any spin qubit and we discuss how to mitigate it by sample design and field orientation.

DOI: 10.1103/PhysRevB.96.180408

## I. INTRODUCTION

In solid-state systems, interactions between electronic spins and their environment are the limiting factor of spin phase lifetime, or decoherence time. Important advances have been recently realized in demonstrating long-lived spin coherence via spin dilution [1–6] and isolating a spin in nonmagnetic cages [7], for instance. The presence of a lattice can be felt by spins through orbital symmetries and spin-orbit coupling. An isolated free electron has a spin angular momentum associated with a $g$ factor $g_e = 2.002\,32$ but in general, spin-orbit coupling changes the $g$ factor by the admixture of excited orbital states [8] into the ground state. In this Rapid Communication, we demonstrate that fluctuations in the spin-orbit interaction can be a significant source of spin decoherence. We present a general theoretical framework to obtain a noise spectrum. The method is applied to fluctuations of the long-range dipolar interactions and we observe how the spin-orbit term is modulating the induced decoherence. The model describes spin dilution and thermal excitations effects as well. Experimentally, we analyze the shape and orientation anisotropy of electron spin resonance (ESR) linewidths of the molecular compound $K_6[V^{IV}_{15}As^{III}_6O_{42}(D_2O)] \cdot 8D_2O$ or $V_{15}$. This system has shown spin coherence at low temperatures [5,9] and interesting out-of-equilibrium spin dynamics due to phonon bottlenecking [10,11]. However, the details of the spin decoherence are still not fully understood. In the case of diluted or molecular spins, little evidence has been brought up to now on the role of spin-orbit coupling on spin coherence time. This study elucidates this decoherence mechanism and how to mitigate its effect.

## II. FLUCTUATIONS IN SPIN HAMILTONIAN

The $V_{15}$ cluster anions form a lattice with trigonal symmetry containing two clusters per unit cell [12]. Individual molecules have 15 $V^{IV}$ $s = 1/2$ ions arranged into three layers—two nonplanar hexagons sandwiching a triangle [see Fig. 1(a)]. Exchange couplings between the spins in the triangle and hexagons exceed 100 K [13,14] and at low temperatures this spin system can be modeled as a triangle of spins 1/2. The spin Hamiltonian is, as discussed in the Supplemental Material (SM), Sec. I [15],

$$\mathcal{H}_{st} = \mathcal{H}_0 + \mathcal{H}_J + \mathcal{H}_{\rm DM}, \tag{1}$$

where $\mathcal{H}_0$ describes the Zeeman splitting in an external field $\vec{B}_0$, $\mathcal{H}_J$ is the symmetric exchange term, and $\mathcal{H}_{\rm DM}$ is the antisymmetric Dzyaloshinsky-Moriya (DM) term (see [16] for a detailed formulation). $\mathcal{H}_{st}$ eigenvalues are shown in Fig. 1(b) and are used to calculate resonant field positions $B_{\rm res}$ of the ESR spectra through the method of first moments [16]. As shown in Fig. 1(b), the ground state of the total molecular spin $\vec{S}$ is $S = 3/2$ for large enough $\vec{B}_0$. In this case, dipolar interactions between total molecular spins in the crystal are described by

$$\mathcal{H}_d = \frac{3\mu_0}{8\pi} S^2 \mu_B^2 \sum_{p;q\neq p} g_p(\theta) g_q(\theta) \frac{(1 - 3\cos^2\phi_{pq})}{d^3_{pq}}, \tag{2}$$

where $\mu_0$ is the vacuum permeability, $\mu_B$ is the Bohr magneton, $\theta$ is the angle between $\vec{B}_0$ and the $z$ axis ($z$ is $\perp$ to triangle plane and is also the symmetry $c$ axis of the molecule), $d_{pq}$ is the distance between two molecules located at sites $p$ and $q$, $g_{p,q}(\theta) = (g_a^2 \sin^2\theta + g_c^2 \cos^2\theta)^{1/2}$, $g_{c,a}$ are the $g$-tensor components parallel and perpendicular to the $z$ axis, and $\phi_{pq}$ is the angle between $\vec{S}$ at site $p$ and $\vec{d}_{pq}$. Due to local fluctuations of the $g$ factor, as discussed below, $g_p$ and $g_q$ are distinct quantities.

The linewidth of ESR signals can be significantly affected by exchange interactions. In $V_{15}$ the intramolecular couplings are large and the exchange narrowing effect [17] collapses the $(2I+1)^{15}$ resonances ($I = 7/2$ for $^{51}$V) into one and it also acts to average out fluctuations related to $\mathcal{H}_{st}$. This leaves fluctuations in $\mathcal{H}_d$ as being the major contributor to spin decoherence.

There are three possible sources of fluctuation in Eq. (2), the first being the geometrical factor $(1 - 3\cos^2\phi_{pq})d^{-3}_{pq} = R_{pq}(t)$ since both $d_{pq}$ and $\phi_{pq}$ can fluctuate (here, $t$ represents time). This case is described by Bloembergen *et al.* [18]

*mmartens@fsu.edu
†ic@magnet.fsu.edu

 

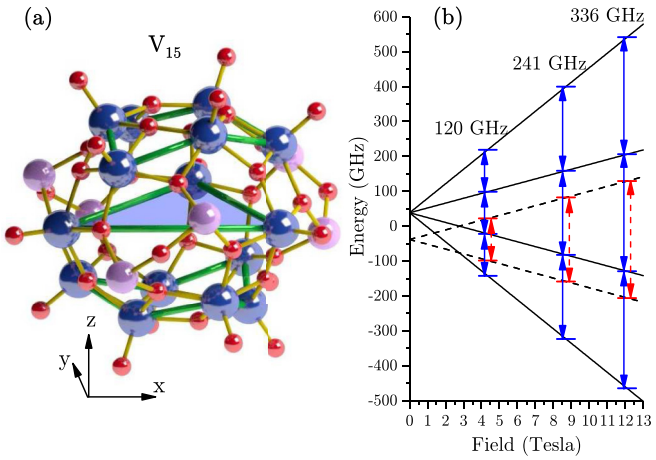


FIG. 1. (a) Ball-and-stick representation of $V_{15}$ (V ions in blue). The $x$ axis is along one side of the triangle, while the $z$ axis is perpendicular to the triangle plane and represents the $c$ axis of the crystal unit cell. (b) Level diagram of the three-spin model in field $\| z$, with positions of the three experimental frequencies shown. Dashed lines show the $S = 1/2$ doublets with the red dashed arrows indicating those transitions. Lines show the $S = 3/2$ quartet with blue arrows indicating the transitions; the resonance fields are averaged in the first moment calculation of $B_{\rm res}$ at a given frequency.

(nuclear magnetic resonance case) and Kubo and Tomita [17] (ESR case). If $R_{pq}(t)$ fluctuates randomly, its correlation function decays exponentially $\langle R(t)R(0)\rangle = R^2 + r^2\exp(-t/\tau_{\rm dip})$ with a Fourier spectrum:

$$J_R(\nu) = \sqrt{\frac{2}{\pi}}r^2\frac{\tau_{\rm dip}}{1+4\pi^2\nu^2\tau_{\rm dip}^2}, \tag{3}$$

where $R$ is an average value of the geometric term $\sum_{p\neq q} R_{pq}$, $r$ is an average size of $R(t)$'s fluctuations, and the correlation time $\tau_{\rm dip}$ is a characteristic of the random motion. This result is described generally by Atherton [19] and can be applied to any stationary random function that is independent of the time origin. The inverse square of the decoherence time $T_2$ is proportional to $\int J_R(\nu)d\nu$ [17,18]. Therefore, the decoherence rate depends directly on $r$: $1/T_2 \propto r$.

Another fluctuation source comes from thermal excitations to different $S_Z$ states of $\vec{S}$, where the $Z$ axis is $\| \vec{B}_0$, which defines the second moment of a resonance line [20–22] (potential fluctuations between different spin states in low fields has been studied as well [9]): $\langle S_Z(t)^2 S_Z(0)^2\rangle = S_Z^4 + KU(T)\exp(-t/\tau_s)$, where $\tau_s$ is the thermal correlation time and $KU(T)$ a term studied by Kambe and Usui [21]. It is shown that the fluctuations Fourier spectrum is proportional to a temperature-dependent factor:

$$KU(T) = \langle S_Z^2\rangle_T - \langle S_Z\rangle_T^2 = S^2\frac{d}{dy}B_s(y), \tag{4}$$

where $B_s(y)$ is the Brillouin function, $y = T_Z S/T$, $T_Z = hf_0/k_B$ ($f_0$ is the microwave excitation frequency), and $S = 3/2$ is the total spin state. $KU(T)$ has thus a similar role to $r^2$ in Eq. (3). This formulation is valid above the ordering temperature which is $\sim$0.01 K [23] for $V_{15}$.

The dipolar term $\mathcal{H}_d$ serves as an excellent platform to study fluctuations of $g(\theta)$. Its value away from $g_e$ is due to the spin-orbit interaction and it is given by [8]

$$\boldsymbol{g} = g_e\boldsymbol{I} - 2\lambda\boldsymbol{\Lambda}, \tag{5}$$

where $\boldsymbol{g}$ is the $g$ tensor (diagonal $[g_a,g_a,g_c]$ for $V_{15}$), $\boldsymbol{I}$ is the unit matrix, $\lambda$ is the spin-orbit coupling constant, and $\boldsymbol{\Lambda}$ is a tensor defined in terms of the matrix elements of the orbital angular momentum $\mathbf{L}$. In general terms, $\Lambda$ is the coupling between the ground and excited orbitals divided by their energy separation. Relative fluctuations with an average size $\xi = \delta(\lambda\Lambda)/(\lambda\Lambda)$ (assumed isotropic) can be induced by crystal and molecular vibrations. In particular, Raman measurements on $V_{15}$ [24] discussed below, show a broad distribution of the vibration modes. Fluctuations of excited orbitals and thus of $\Lambda$ can generate broad virtual transitions since those orbitals are mixed with the ground orbital state. The resultant fluctuation in the $g$ factor can be written as

$$\delta g(\theta) = \xi[g(\theta) - g_e]. \tag{6}$$

Assuming $g(\theta)$ is a stationary function with small temporal random fluctuations and that magnetic and orbital fluctuations are uncorrelated in first approximation, the correlation function of a fluctuating $\mathcal{H}_d(t)$ is

$$\begin{aligned} G_d(t) &= \langle\mathcal{H}_d(t)\mathcal{H}_d(0)\rangle \\ &= \alpha^2\langle g(t)g(0)\rangle^2\langle S_Z^2(t)S_Z^2(0)\rangle\langle R(t)R(0)\rangle, \end{aligned} \tag{7}$$

where $\langle g(t)g(0)\rangle = g(\theta)^2 + [\delta g(\theta)]^2\exp(-t/\tau_g)$, $\tau_g$ is the correlation time of $g$-factor fluctuations, and $\alpha = \frac{3\mu_0\mu_B^2}{8\pi}$. A corresponding $J_d(\nu)$ gives the Fourier spectrum of the fluctuations, as in Eq. (3). $G_d(t)$ can be written as the sum of four terms (see SM, Sec. II, for details): $G_0$ which is a constant, $G_g(t) \propto g(\theta)^4$, $G_\delta(t)$ which is temperature independent, and $G_T(t)$ which is temperature dependent.

In absence of $g$-factor fluctuations, the resulting Fourier spectrum is defined only by $G_g(t)$ and for negligible $r$ (less important in solids at low temperatures) the term $G_g(t) \approx \alpha^2 g(\theta)^4 R^2 KU(T)e^{-(t/\tau_s)}$ is as in [21]. A temperature dependence of the linewidth $\propto KU(T)$ is similar to observations done with $Fe_8$ [25–27], nitrogen-vacancy color centers in diamond [28], while other studies seem to confirm the proportionality to the $g$ factor [29,30]. If the $g$ value does fluctuate, then all three terms $G_{g,\delta,T}$ represent sources of decoherence, with $G_\delta + G_T$ given by

$$\begin{aligned} G_\delta(t) + G_T(t) \approx{}& \alpha^2R^2[S^4 + KU(T)] \\ &\times [2g(\theta)^2\delta g^2(\theta)e^{-(t/\tau_g)} + \delta g^4(\theta)e^{-(2t/\tau_g)}]. \end{aligned} \tag{8}$$

Because $1/T_2^2$ is $\propto\int J_d(\nu)d\nu$, an important consequence is that one can combine different decoherence sources by summing their effect (each term $i$) as follows: $\frac{1}{T_2^2} \approx \sum_i \frac{1}{T_{2i}^2}$, similar to the well-known fact that the sum of uncorrelated variances is equal to the total variance. Additionally, the weight of each term in the sum depends on, or can be tuned with, the field angle $\theta$ through $g$ and $\delta g$. Here we show that for $V_{15}$, the anisotropy of the decoherence time is explained by fluctuations $\delta g$, as shown in Eq. (8), amplified by spin thermal fluctuations $KU(T)$.

### III. EXPERIMENTAL DATA

Continuous-wave ESR measurements at 120, 241, and 336 GHz are performed using the quasioptical superheterodyne spectrometer at the National High Magnetic Field Laboratory [31,32], with a sweepable 12.5 T superconducting magnet (homogeneity of $10^{-5}$ over 1 $cm^3$). Sample temperatures can be varied from room temperature down to 2.5 K. A single crystal of regular shape (as in [16]) of volume $\lesssim 0.1$ $mm^3$ was positioned on a rotating stage allowing for continuous change of the angle $\theta$ between $\vec{B}_0$ and the $c$ axis of the molecule following the procedure described in [16]. The homogeneity of the magnet compared to the size of the crystal allows us to ignore $\vec{B}_0$ as a source of broadening. The applied fields are above 4 T, past the crossing of the $S = 1/2$ doublet and $S = 3/2$ quartet, such that the ground state of the system is in the $S = 3/2$ quartet [see Fig. 1(b)].

ESR spectra at temperatures $T = 4$–60 K for $\vec{B}_0 \parallel$ and $\perp$ to the $c$ axis ($\theta = 0\circ, 90\circ$, respectively) show a Lorentzian (homogenous) line shape. Representative spectra with Lorentzian and Gaussian fits are shown in Fig. 2(a) for comparison. The temperature dependence of the linewidth is shown in Fig. 2(c) for three microwave frequencies $f_0$. Compared to measurements made at lower fields [33], where the ground state is in the $S = 1/2$ doublet, the linewidths are approximately ten times narrower. Plotted is the FWHM of the Lorentzian fits vs $T/f_0$ to underline that the temperature-dependent mechanism of decoherence in the system qualitatively follows the temperature behavior predicted by $KU(T)$ plus a temperature-independent contribution, essential in the low $T$ limit [Eq. (8)]. Note the absence of linewidth increase with frequency (or field) which excludes a static distribution of the $g$ factor. Additionally, there is no hyperfine structure visible in the spectra (exchange narrowing) since the $3d$ electrons of V interact with the nuclei of several other V ions due to the large exchange couplings ($\sim 10^2$ K) within the molecule. Due to these properties of the measured line-width and shape, we can estimate $T_2$ to be the inverse of the FWHM.

There are two distinct curves in Fig. 2(c), dependent on the orientation of $\vec{B}_0$. To probe this orientation dependence, the linewidth is measured as a function of $\theta$ [see Fig. 2(b)]. The narrowest linewidth occurs when $\theta = 0^\circ$ ($\vec{B}_0 \parallel c$ axis), while the largest occurs at $\theta = 90^\circ$ ($\vec{B}_0$ in the triangle plane). This implies more decoherence the further $g(\theta)$ gets from $g_e$ since $g(0^\circ) = g_c \approx 1.98$ and $g(90^\circ) = g_a \approx 1.95$. The fact that the width is largest (smallest) when $g(\theta)$ is minimum (maximum) rules out exchange narrowing being the cause of this anisotropy since it would require a linewidth $\propto (1 + \cos^2\theta)$ [17], as in the case of $CsCuCl_3$ [34]. To rule out an angular effect of the dipolar field distribution, we measured the FWHM($\theta$) on a sample of irregular shape at 240 GHz and 60 K. Although the shape-dependent coefficients $R$ and $r$ must be different, the same behavior is observed as in Fig. 2(b) (see SM, Sec. III B for details). We can thus focus on the terms $G_{g,\delta,T}$ as the source of fluctuations.

However, the term $G_g(t)$ is $\propto g(\theta)^4$, in clear contrast with the observation that the FWHM and $g(\theta)$ have opposite angular dependences [see Fig. 2(b) and also SM, Sec. III A). This is the essential property of the $V_{15}$ compound, which makes it particularly suitable to study the effect of

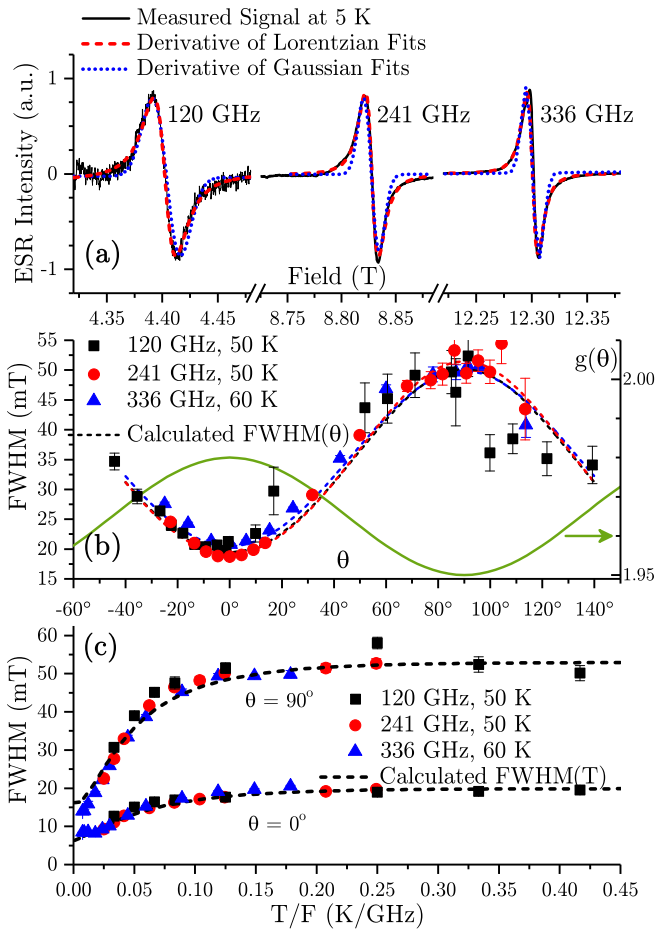


FIG. 2. (a) Typical measurements of the derivative of the absorption $\chi''$ at 120, 241, and 336 GHz with derivatives of Gaussian (blue dotted line) and Lorentzian (red dashed line) fits. (b) FWHM of Lorentzian fits as a function of field angle $\theta$ measured at three frequencies: 336 GHz (blue triangles), 241 GHz (red circles), and 120 GHz (black squares). The dashed lines are calculated widths as a function of $\theta$; the agreement shows the predicted correlation between the decoherence rate and $g_e - g(\theta)$. In contrast, the green line (right axis) shows the opposite angular behavior of calculated $g(\theta)$, leading to $G_g \ll G_\delta + G_T$ (see text). (c) FWHM of Lorentzian fits vs temperature/frequency for the three studied frequencies. Dashed lines are calculated FWHM($T$) for $\theta = 0^\circ$ and $90^\circ$.

spin-orbit fluctuations. Therefore, this opposite angular behavior provides evidence that $\delta g(\theta) \neq 0$ and the terms $G_{\delta,T}(t)$ must be considered, while $G_g(t)$ can be discarded. One can argue that geometrical fluctuations in solids at low temperatures are very small ($r \ll R$) and lattice fluctuations are mostly influencing the relaxation time $T_1$ ($\tau_s \gg \tau_g$) making $G_g \approx$ constant at the time scale of the decoherence time.

Since $G_d(t) \approx G_\delta(t) + G_T(t)$ and $1/T_2^2 \propto \int J_d(\nu)$ [17,18] the linewidth square can be modeled by the following fit function (see SM, Sec. II for details):

$$\Delta^2 = [S^4 + KU(T)] \times \{2a^2 g(\theta)^2 [g(\theta) - g_e]^2 + A^2 [g(\theta) - g_e]^4\}, \quad (9)$$

where $A$ and $a$ are fit parameters. The procedure is detailed in SM, Sec. IV; it allows one to calculate the angular dependence FWHM($\theta$) by using only two data points, $\Delta(0^\circ)$ and $\Delta(90^\circ)$, as shown in Fig. 2(b) (dashed lines).

To analyze the temperature dependence of the linewidth shown in Fig. 2(c), we solve for $A$ and $a$ at all available temperatures and frequencies (see SM, Sec. IV B for details). Above 10–20 K, the values stabilize at $A \sim 100$ GHz and $a \sim 3.2$ GHz. At lower temperatures, the values decrease by almost half, indicating a small decrease in $\xi$ and/or a slowing down in the fluctuation time $\tau_g$. These temperature trends $A(T)$ and $a(T)$ are estimated by an exponential saturation (see SM, Fig. 4 for details), with decay constants of 3.6 and 11 K for $A(T)$ and $a(T)$, respectively. With no other adjustments, the calculated linewidth is in very good agreement with the experimental data, as shown by the dashed line in Fig. 2(c). On the low end of $T/f_0$ one observes a residual value of the linewidth, which includes the effects of other decoherence sources (such as the nuclear spin bath [35]), although it can be well described by Eq. (9).

The outcome of the fit procedure can be used to estimate the size of spin-orbit fluctuations (see SM, Sec. IV C) leading to an order of magnitude for $\xi \sim 10^{-2}$. This corresponds to a fluctuation $\delta g/g \sim 10^{-4}$, too small to result in directly measurable fluctuations of the Zeeman splitting. Note that for $V_{15}$, a large spin-orbit fluctuation is supported by previous Raman measurements [24] showing a very broad signal in the region of $\sim$500 cm$^{-1}$ corresponding to vibrations of oxygen bridges between V ions. The observed broad distribution of the modes can induce very fast virtual transitions to excited coupled states and, as a consequence, spin decoherence.

## IV. CONCLUSION

Our study provides insight on how to mitigate the effects of spin-orbit fluctuations. It is evident from Eqs. (6) and (7) that the $g$ tensor should be as close as possible to $g_e$. In molecular compounds this can be achieved by engineering the ligands type since local symmetry affects the diagonal values of the $g$ tensor of a magnetic ion. Aside from material design by chemical methods, $J_d(\nu)$ can be minimized by applying the magnetic field at a specific angle $\theta$. For $V_{15}$, this would be $\theta = 0$ for which the decoherence time reaches several nanoseconds. This time can reach $\sim$400 ns by reducing $R$ in $J_d(\nu)$ via dilution in liquid state, thus allowing the observation of Rabi oscillations and spin echoes [5]. The methodology presented here can be important for the diluted spin systems as well, since long-range interactions are still present and can carry modulations due to $g$-factor fluctuations. Potential examples are transition metals such as $Cr^{5+}:K_3NbO_8$ [2]) or some lanthanide monomers doped into insulating lattice such as $Hf:LuPO_4$ [36] or $La:CaF_2$ [37]. The results extend to any solid-state system where spin-orbit coupling leads to quantum effects, independent of system dimensionality.

## ACKNOWLEDGMENTS

We wish to acknowledge David Zipse and Vasanth Ramachandran for their help in growing $V_{15}$ crystals. This work was supported by NSF Grant No. DMR-1206267 and CNRS-PICS CoDyLow. The NHMFL is supported by Cooperative Agreement Grant No. DMR-1157490 and the state of Florida. The experiments were performed at the EPR facilities of the NHMFL, and we thank Dr. Johan van Tol for his support.

[1] S. Bertaina, L. Chen, N. Groll, J. Van Tol, N. S. Dalal, and I. Chiorescu, Phys. Rev. Lett. **102**, 050501 (2009).
[2] S. Nellutla, K.-Y. Choi, M. Pati, J. van Tol, I. Chiorescu, and N. S. Dalal, Phys. Rev. Lett. **99**, 137601 (2007).
[3] S. Bertaina, S. Gambarelli, A. Tkachuk, I. N. Kurkin, B. Malkin, A. Stepanov, and B. Barbara, Nat. Nanotechnol. **2**, 39 (2007).
[4] M. V. G. Dutt, L. Childress, L. Jiang, E. Togan, J. Maze, F. Jelezko, A. S. Zibrov, P. R. Hemmer, and M. D. Lukin, Science **316**, 1312 (2007).
[5] S. Bertaina, S. Gambarelli, T. Mitra, B. Tsukerblat, A. Müller, and B. Barbara, Nature (London) **453**, 203 (2008).
[6] A. Ardavan, O. Rival, J. J. L. Morton, S. J. Blundell, A. M. Tyryshkin, G. A. Timco, and R. E. P. Winpenny, Phys. Rev. Lett. **98**, 057201 (2007).
[7] G. W. Morley, J. van Tol, A. Ardavan, K. Porfyrakis, J. Zhang, and G. A. D. Briggs, Phys. Rev. Lett. **98**, 220501 (2007).
[8] M. H. L. Pryce, Proc. Phys. Soc., London, Sect. A **63**, 25 (1950).
[9] V. V. Dobrovitski, M. I. Katsnelson, and B. N. Harmon, Phys. Rev. Lett. **84**, 3458 (2000).
[10] I. Chiorescu, W. Wernsdorfer, A. Müller, H. Bögge, and B. Barbara, J. Magn. Magn. Mater. **221**, 103 (2000).
[11] I. Chiorescu, W. Wernsdorfer, A. Müller, H. Bögge, and B. Barbara, Phys. Rev. Lett. **84**, 3454 (2000).
[12] A. Müller and J. Döring, Angew. Chem., Int. Ed. Engl. **27**, 1721 (1988).
[13] D. Gatteschi, L. Pardi, A. L. Barra, A. Müller, and J. Döring, Nature (London) **354**, 463 (1991).
[14] A. L. Barra, D. Gatteschi, and L. Pardi, J. Am. Chem. Soc. **114**, 8509 (1992).
[15] See Supplemental Material at http://link.aps.org/supplemental/10.1103/PhysRevB.96.180408 for details on theoretical calculations and simulations as well as supporting additional data.
[16] M. Martens, J. van Tol, N. S. Dalal, S. Bertaina, B. Barbara, B. Tsukerblat, A. Müller, S. Garai, S. Miyashita, and I. Chiorescu, Phys. Rev. B **89**, 195439 (2014).
[17] R. Kubo and K. Tomita, J. Phys. Soc. Jpn. **9**, 888 (1954).
[18] N. Bloembergen, E. M. Purcell, and R. V. Pound, Phys. Rev. **73**, 679 (1948).
[19] N. M. Atherton, *Electron Spin Resonance: Theory and Applications* (Wiley, New York, 1973).
[20] M. H. L. Pryce and K. W. H. Stevens, Proc. Phys. Soc., London, Sect. A **63**, 36 (1950).
[21] K. Kambe and T. Usui, Prog. Theor. Phys. **8**, 302 (1952).
[22] M. McMillan and W. Opechowski, Can. J. Phys. **38**, 1168 (1960).
[23] B. Barbara, I. Chiorescu, W. Wernsdorfer, H. Bögge, and A. Müller, Prog. Theor. Phys. Suppl. **145**, 357 (2002).
[24] D. Zipse, N. S. Dalal, R. Vasic, J. S. Brooks, and P. Kögerler, Phys. Rev. B **71**, 064417 (2005).
[25] K. Park, M. A. Novotny, N. S. Dalal, S. Hill, and P. A. Rikvold, Phys. Rev. B **66**, 144409 (2002).

[26] S. Hill, S. Maccagnano, K. Park, R. M. Achey, J. M. North, and N. S. Dalal, Phys. Rev. B **65**, 224410 (2002).

[27] S. Takahashi, J. van Tol, C. C. Beedle, D. N. Hendrickson, L.-C. Brunel, and M. S. Sherwin, Phys. Rev. Lett. **102**, 087603 (2009).

[28] S. Takahashi, R. Hanson, J. van Tol, M. S. Sherwin, and D. D. Awschalom, Phys. Rev. Lett. **101**, 047601 (2008).

[29] M. J. Graham, J. M. Zadrozny, M. Shiddiq, J. S. Anderson, M. S. Fataftah, S. Hill, and D. E. Freedman, J. Am. Chem. Soc. **136**, 7623 (2014).

[30] S. Takahashi, I. S. Tupitsyn, J. van Tol, C. C. Beedle, D. N. Hendrickson, and P. C. E. Stamp, Nature (London) **476**, 76 (2011).

[31] G. W. Morley, L.-C. Brunel, and J. van Tol, Rev. Sci. Instrum. **79**, 064703 (2008).

[32] J. van Tol, L.-C. Brunel, and R. J. Wylde, Rev. Sci. Instrum. **76**, 074101 (2005).

[33] T. Sakon, K. Koyama, M. Motokawa, Y. Ajiro, A. Müller, and B. Barbara, Phys. B (Amsterdam, Neth.) **346-347**, 206 (2004).

[34] H. Tanaka, K. Iio, and K. Nagata, J. Phys. Soc. Jpn. **50**, 727 (1981).

[35] N. V. Prokof'ev and P. C. E. Stamp, Phys. Rev. Lett. **80**, 5794 (1998).

[36] M. M. Abraham, L. A. Boatner, and J. O. Ramey, J. Chem. Phys. **83**, 2754 (1985).

[37] W. Hayes and J. W. Twidell, Proc. Phys. Soc. **82**, 330 (1963).